PHYSICAL REVIEW A **93**, 043424 (2016)

Lifetimes of metastable ion clouds in a Paul trap: Power-law scaling

D. K. Weiss, Y. S. Nam, and R. Blümel
Department of Physics, Wesleyan University, Middletown, Connecticut 06459-0155, USA
(Received 30 July 2015; revised manuscript received 23 September 2015; published 27 April 2016)

It is well known that ions stored in a Paul trap, one of the most versatile tools in atomic, molecular, and optical (AMO) physics, may undergo a transition from a disordered cloud state to a geometrically well-ordered crystalline state, the Wigner crystal. In this paper we predict that close to the transition, the average lifetime $\bar{\tau}_m$ of the metastable cloud follows a power law, $\bar{\tau}_m \sim (\gamma - \gamma_c)^{-\beta}$, where γ_c is the value of the damping constant at which the transition occurs. The exponent β depends on the trap control parameter q, but is independent of both the number of particles N stored in the trap and the trap control parameter a, which determines the shape (oblate, prolate, or spherical) of the ion cloud. In addition, we find that for given a and q, γ_c scales approximately like $\gamma_c = C\ln[\ln(N)] + D$ as a function of N, where C and D are constants. Our predictions may be tested experimentally with equipment already available at many AMO laboratories. In addition to their importance in AMO trap physics, we also discuss possible applications of our results to other periodically driven many-particle systems, such as, e.g., particle accelerator beams, and, based on our trap results, conjecture that power laws characterize the phase transition to the Wigner crystal in all such systems.

DOI: 10.1103/PhysRevA.93.043424

I. INTRODUCTION

The Paul trap [1,2] is an electrodynamic device for storing charged particles free from contact with material walls for very long periods of time. Trapping is achieved by applying suitable dc and ac voltages to the hyperbolic electrodes of the trap. The resulting electric potentials create an effective potential minimum at the center of the trap, an immaterial trough that confines charged particles, in principle, forever. Storage times ranging from a few hours [3] to a few days [4] have been reported.

One of the most interesting phenomena that has attracted considerable interest in the atomic, molecular, and optical (AMO) community for some time is the observation that ions stored in a Paul trap can occur in two completely different states, a well-ordered crystalline state [5–15], also called the Wigner crystal [10,13,16], and a disordered cloud state [17–20]. Experimentally observed transitions between these two states [3,4,21–24], as well as their theoretical interpretations [3,15,21,25], have also attracted attention in the AMO community. Technological applications of ion crystals are now emerging. For instance, linear and higher-dimensional ion crystals have been proposed as quantum hardware components for quantum computers [9,10].

Theoretically and experimentally, trapping of a single charged particle in an ideal Paul trap is understood in detail [1,2], and even its quantum regime has already been explored [26,27]. However, if multiple particles are stored in the trap simultaneously, the Coulomb interactions between the particles cause their motions to be chaotic [2,3,28,29]. In this case it is no longer possible to solve their equations of motion analytically. The chaotic motion of the particles has two consequences. (i) Due to the resulting high temperatures, we do not have to worry about quantum effects; a classical description of the trapped particles is sufficient. (ii) The chaotic motion of the particles in the trap causes the phenomenon of radio-frequency (rf) heating [3,19–21,30,31]. Damping must be imparted to this system to counteract the heating, whether through laser cooling [3], buffer gas cooling [4], or some other method, for instance, cooling by the cold, neutral particles of a magneto-optic trap [32]. With a relatively small damping, the rf heating power of the ion cloud will come into equilibrium with the cooling power, resulting from the damping mechanism, and a stationary-state gas cloud will result [3,19–21]. However, with stronger damping, the heating of the cloud can be overcome, and the particles will transition into the crystalline state [3,4,22–24].

In this paper we use large-scale molecular dynamics simulations to predict that close to the cloud $\rightarrow$ crystal transition the lifetimes of ion clouds stored in a Paul trap follow a power law, which may be tested experimentally with equipment available at many AMO laboratories. We also obtain a scaling law for the critical amount of damping required to collapse ion clouds into ion crystals.

Our paper is organized as follows. In Sec. II we present the equations that govern the motion of ions in a Paul trap together with our method of solving these equations and extracting lifetime information from our molecular-dynamics simulations. In Sec. III we present the results of our molecular-dynamics simulations that lead us directly to our two main predictions, i.e., the power-law scaling of the lifetimes of metastable clouds and the scaling of the critical damping required to force the transition from the cloud state into the crystal state. In Sec. IV we discuss our results and their potential applications in a broad class of periodically driven multiparticle systems, such as particle accelerator beams [33,34], dusty plasmas [35,36], surface state electrons [37], and colloidal suspensions [38,39]. We summarize and conclude our paper in Sec. V.

II. THEORY AND METHODS

The coupled equations of motion governing the dynamics of N particles stored in the Paul trap, in dimensionless units [19], are

$$\ddot{\vec{r}}_i + \gamma\dot{\vec{r}}_i + [a - 2q\sin(2\tau)]\begin{pmatrix} x_i \\ y_i \\ -2z_i \end{pmatrix} = \sum_{\substack{j=1 \\ j\neq i}}^{N} \frac{\vec{r}_i - \vec{r}_j}{|\vec{r}_i - \vec{r}_j|^3}, \quad i = 1,\ldots,N, \tag{1}$$

where $\vec{r}_i = (x_i,y_i,z_i)$ is the position vector of ion number i, τ is the dimensionless time, γ is the damping constant, N is the number of trapped particles, and a,q are the trap's dimensionless control parameters [19], proportional to the dc and ac voltages applied to the trap's electrodes, respectively. The conversion between time τ and the number n of rf cycles is accomplished via $n = \tau/\pi$. For given values of N, a, q, and γ, we solve (1) numerically with a standard fifth-order Runge-Kutta integrator [40]. Each of our simulations starts at $\tau = 0$ with randomly chosen initial conditions drawn from the phase-space box $-10 < x,y,z < 10$, $-1 < v_x,v_y,v_z < 1$ with a uniform distribution. We checked that, because of the chaotic nature of the particle dynamics in the trap, all of our results are completely insensitive to both the particular choice of random distribution and the size of the box. To monitor the progress of our simulations, we plot $\langle x^2(\tau_n = n\pi)\rangle = \sum_{i=1}^{N} x_i^2(\tau_n = n\pi)$, n integer.

III. RESULTS

The result of a typical simulation run is shown in Fig. 1. Since they are chosen at random, all of our initial conditions correspond to energetic particle clouds with large initial values of $\langle x^2\rangle$ (see data points for $\tau \approx 0$ in Fig. 1). However, because of the chaotic nature of its dynamics, the particle cloud very quickly loses the memory of its initial conditions and thermalizes. This corresponds to the initial transient [see the near-exponential decay over the first $\sim$1000 rf cycles ($\tau \approx 0$ to $\tau \approx 3000$) in Fig. 1], followed by the establishment of a metastable stationary state (see the plateau in Fig. 1 of length $\tau_m \approx 28\,000$), where the heating of the cloud comes into equilibrium with the damping. Following this, if, as in Fig. 1, a relatively large γ was chosen, the cloud eventually collapses into the crystal state. In Fig. 1 this final collapse manifests itself as the exponential decay phase immediately following the metastable state (to the right of the second dashed line in Fig. 1) and ending in the crystalline state, characterized by the absence of fluctuations in $\langle x^2\rangle$ for $\tau \gtrsim 40\,000$. We checked explicitly that during its plateau state the ion cloud is stable in the sense that in addition to $\langle x^2\rangle$ we checked the expectation values of several other dynamical variables, but did not find any that would decay during τ_m.

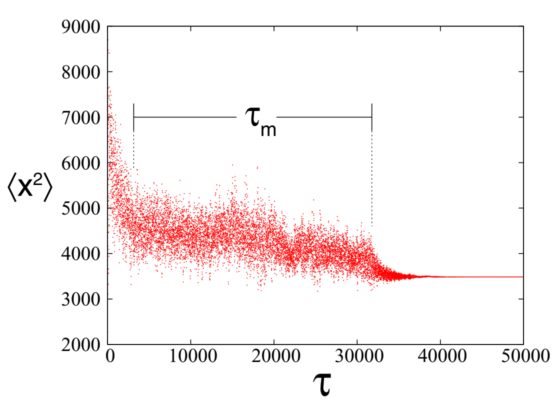

FIG. 1. Square displacement $\langle x^2(\tau)\rangle$ of a 100-particle cloud for $q = 0.2$, $a = 0.02$, and $\gamma = 8.81 \times 10^{-4} > \gamma_c = 8.47 \times 10^{-4}$. An initial transient (thermalization stage) is followed by a plateau of length τ_m (metastable state), which ultimately transitions into a state of constant $\langle x^2(\tau)\rangle$ (flat line; crystalline state).

Confirming previous experimental [3,4] and numerical [3] observations, we find that for given N,a,q the cloud $\to$ crystal transition (the final collapse of the cloud in Fig. 1) occurs in the vicinity of a critical value of γ, denoted by γ_c. In addition, corroborating earlier qualitative experimental observations (see, e.g., Fig. 3 in [3]), we find that, for finite N, and a given finite simulation time $\tau_{\max}$, γ_c is not sharply defined. Therefore, to determine γ_c and its uncertainty, we proceed in the following way. For given N,a,q, we scan γ from $\gamma_{\min} = 10^{-5}$ to $\gamma_{\max} = 2 \times 10^{-2}$, a γ interval that we know from experience contains γ_c with certainty for N ranging between 20 and 2000 trapped particles. We find that in the interval $\gamma_{\min} < \gamma < \gamma_1(N,a,q)$, N-particle clouds are stable and never transition into the crystal. Following this is the interval $\gamma_1(N,a,q) < \gamma < \gamma_2(N,a,q)$, an interval of uncertainty, in which the clouds sometimes transition into the crystal and sometimes not. Adjacent to this is the interval $\gamma_2(N,a,q) < \gamma < \gamma_{\max}$, in which all N-particle clouds, independently of initial conditions, always transition into crystals. Defining $\Delta\gamma_c = \gamma_2 - \gamma_1$ as the width of the uncertainty interval, we find that $\Delta\gamma_c$ shrinks, i.e., γ_1 and γ_2 both move toward each other with increasing number N of stored particles according to $\Delta\gamma_c \sim 1/\sqrt{N}$, and also with the maximal time $\tau_{\max}$ allowed for our simulations. To be practical, however, we limited the run time of our simulations to $\tau_{\max} = 5 \times 10^5\pi$, very much larger than the typical decay time $1/\gamma$ of our system. We found that this choice of $\tau_{\max}$ yielded consistent results, and we saw no need to increase $\tau_{\max}$. Having determined the uncertainty interval $[\gamma_1,\gamma_2]$, we define $\gamma_c = (\gamma_1 + \gamma_2)/2$.

As an example, for $q = 0.2$, $a = q^2/2$, and N ranging from 25 to 1000 particles, we plot, in Fig. 2, the γ_c values (red, closed circles) determined according to the numerical procedure described above. The uncertainty $\Delta\gamma_c$ of γ_c is smaller than the size of the plot symbols in Fig. 2. We found that neither a power law ($\gamma_c = AN^B + C$, where A,B,C are fit parameters; blue, solid line in Fig. 2) nor a log law [$\gamma_c = A\ln(N) + B$, where A,B are fit parameters; green, solid line in Fig. 2] fits the N dependence of γ_c satisfactorily, but that the iterated log law,

$$\gamma_c(N,q = 0.2,a = 0.02) = C\ln[\ln(N)] + D \tag{2}$$

(red, solid line in Fig. 2), provides an excellent fit, where $C = 7.49 \times 10^{-4}$ and $D = -2.97 \times 10^{-4}$. For $N = 100$, $\gamma_c = 8.47 \times 10^{-4}$. This is the reason for why the cloud in Fig. 1, subjected to $\gamma = 8.81 \times 10^{-4} > \gamma_c$, ultimately collapses into the crystal state.

At present, we are not able to provide an analytical explanation for the origin of the iterated-log scaling of γ_c. However, the weak N dependence of γ_c, reflected in its $\ln[\ln(N)]$

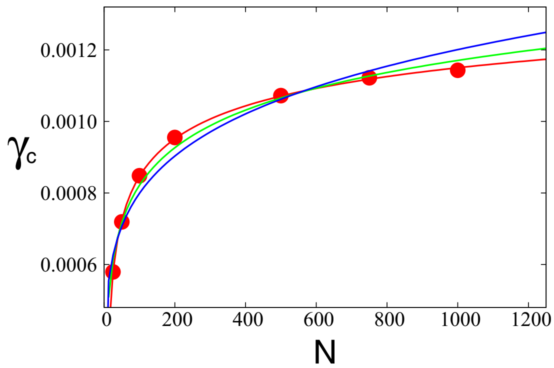

FIG. 2. Critical value $\gamma_c(N,q = 0.2, a = 0.02)$ of the damping constant γ [see (1)] as a function of N at which the cloud → crystal transition occurs (red, closed circles). The best-fitting power law (blue, solid line), log law (green, solid line), and the iterated log law (red, solid line) are also shown. Only the iterated log law, according to (2), provides a satisfactory fit.

scaling, may be understood qualitatively in the following way. Since, in the large-N limit, and close to the cloud → crystal transition, charged particles in the interior of the Paul trap have a near-constant density (similar to a charged liquid in a confining harmonic-oscillator potential), all particles deep in the interior of the trap may be treated as equivalent, since they are experiencing approximately the same homogeneous surrounding charge density. Given that γ represents the energy loss per particle [see (1)], $\gamma_c(N)$ is expected to be constant. Thus, the small deviation of the $\gamma_c(N)$ scaling from constancy, i.e., the presence of the $\ln[\ln(N)]$ term, is a finite-size (surface) effect that is hard to capture analytically.

We now turn to a more in-depth investigation of the cloud → crystal transition, i.e., we focus on the interval $\gamma > \gamma_2 > \gamma_c$. In particular, we are interested in the time it takes for a cloud to crystallize, once it has achieved its metastable state (the plateau in Fig. 1), i.e., we are interested in the length of time τ_m the cloud spends in the metastable state before quickly transitioning into the crystalline state (ultimate exponential decay in Fig. 1). It is intuitively clear that the larger γ, the shorter τ_m. Conversely, when approaching γ_2 from above, and taking into account that clouds are stable for $\gamma < \gamma_1 \approx \gamma_c$, τ_m should increase as γ approaches $\gamma_2 \approx \gamma_c$. This suggests a power law of the form,

$$\tau_m(N,a,q;\gamma) \sim [\gamma - \gamma_c(N,a,q)]^{-\beta(N,a,q)}, \qquad (3)$$

for $\gamma \gtrsim \gamma_c$, where $\beta > 0$. To find β we ran our simulations for fixed N,a,q for γ values that approach $\gamma_c(N,a,q)$ from above and extracted τ_m via an automated, objective process [41]. Since the motion of the particles in the Paul trap is fully chaotic, small changes in the initial conditions can produce different values of τ_m. Therefore, we ran our simulations with 50 different initial conditions and defined $\bar{\tau}_m$ as the average over the 50 resulting τ_m values. To characterize the statistical

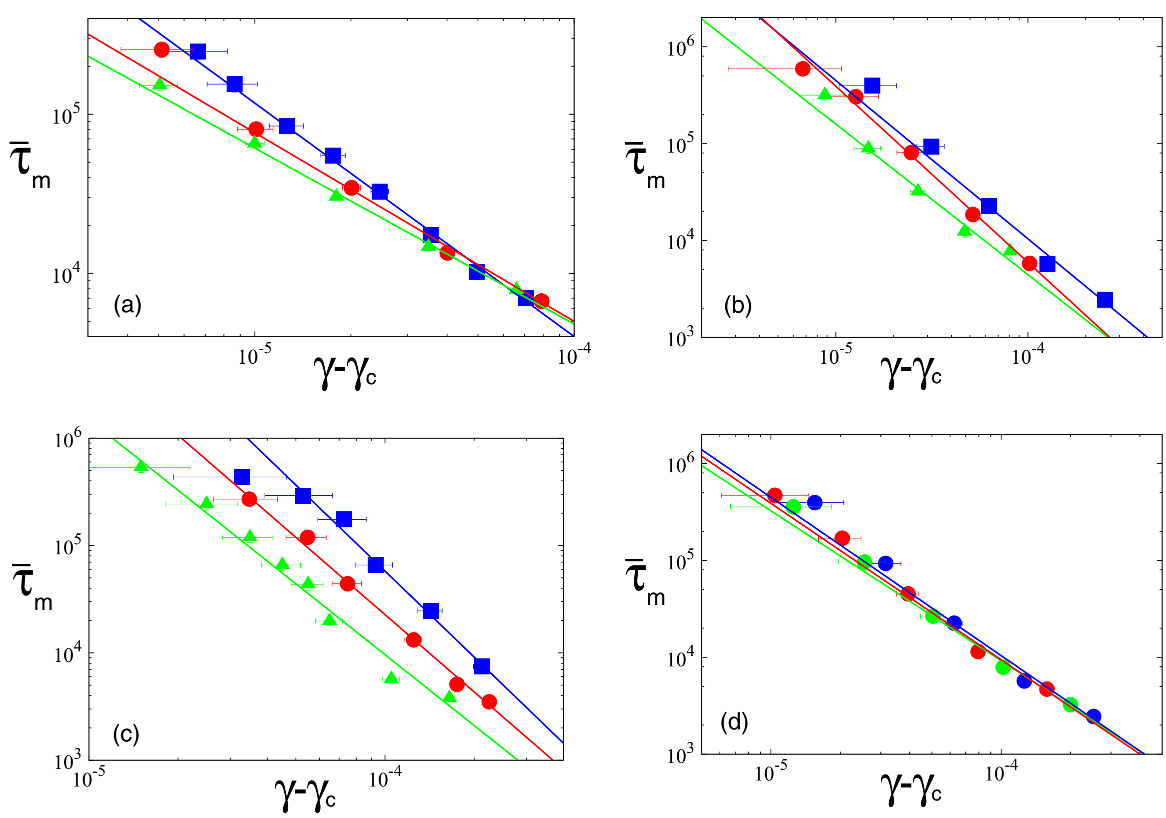

FIG. 3. Average time $\bar{\tau}_m$ spent in the metastable state versus the distance $\gamma - \gamma_c$ from the critical point γ_c. (a) $q = 0.15$, (b) $q = 0.20$, and (c) $q = 0.25$ for the spherical case $a = q^2/2$. Shown are $N = 100,200,500$ (blue, red, green, respectively). (d) $q = 0.20$, where $a = 0$ (oblate, red), $a = q^2/2$ (spherical, blue), and $a = 4q^2/5$ (prolate, green) for $N = 100$. The exponents β and the goodness of the fit, tested according to χ^2 statistics, are available in Table I.

TABLE I. Exponents β and the corresponding goodness-of-fit parameters χ^2 obtained from fitting the power law (3) to the data in Fig. 3. In the case of spherical clouds ($a = q^2/2$), for a given q and several different N, the exponents β lie within the margins of error, with the exception of $q = 0.15$ and $N = 100$, which is an outlier. The exponents β obtained from different shapes of clouds resulting from several different choices of a lie within the margins of error as well. Thus, β is approximately independent of a and N.

	Simulation parameters		β	χ^2
$a = q^2/2$ (spherical)	$q = 0.15$	$N = 100$	1.47 ± 0.13	0.95
		$N = 200$	1.19 ± 0.10	1.00
		$N = 500$	1.11 ± 0.09	0.69
	$q = 0.20$	$N = 100$	1.63 ± 0.19	1.62
		$N = 200$	1.82 ± 0.35	0.08
		$N = 500$	1.55 ± 0.32	0.84
	$q = 0.25$	$N = 100$	2.66 ± 0.69	0.22
		$N = 200$	2.39 ± 0.41	0.34
		$N = 500$	2.19 ± 0.34	1.98
$N = 100, q = 0.2$	$a = 0$	(oblate)	1.62 ± 0.23	0.83
	$a = q^2/2$	(spherical)	1.63 ± 0.19	1.62
	$a = 4q^2/5$	(prolate)	1.55 ± 0.24	0.39

spread of the τ_m values, we also computed the standard error $\alpha = [(1/50)\sum_{j=1}^{50}(\tau_m^{(j)} - \bar{\tau}_m)^2]^{1/2}/\sqrt{50}$. For $q = 0.15$, 0.20, and 0.25 and $a = q^2/2$ (spherical clouds), Figs. 3(a)–3(c) show the resulting dependence of $\bar{\tau}_m$ on $(\gamma - \gamma_c)$ (plot symbols). The length of the horizontal error bars in Fig. 3 equals $\Delta\gamma_c$. The vertical error bars in Fig. 3, of length α, are smaller than the plot symbols. If (3) holds, the data in Fig. 3 should fall on straight lines. According to Fig. 3, this is indeed the case.

Following [40], we extracted the exponents β of the power law (3) from the data presented in Fig. 3 according to the following procedure. We define

$$\chi^2(d,\beta) = \sum_{i=1}^{\nu} \frac{(\eta_i - d - \beta\xi_i)^2}{\sigma_{\eta i}^2 + \beta^2\sigma_{\xi i}^2}, \tag{4}$$

where, for given N,a,q, i counts the ν data points available in each data set, $\eta_i = \ln(\bar{\tau}_{mi})$, $\xi_i = \ln(\gamma_i - \gamma_c)$, $\sigma_{\eta i} = \Delta\eta_i = \alpha_i/\bar{\tau}_{mi}$, and $\sigma_{\xi i} = \Delta\xi_i = \Delta\gamma_c/(\gamma_i - \gamma_c)$. The intercept d and the exponent β are then obtained by minimizing (4) with respect to d and β. We report the β values and associated χ^2 values obtained at the χ^2 minima in Table I. The χ^2 values are all of the order or smaller than 1, indicating that the straight-line fits in Fig. 3 are meaningful. The uncertainties in β were computed according to formula 15.3.5 of [40] as the extrema of the error ellipse defined by the second derivatives of χ^2 with respect to d and β. The values of the uncertainties in β, obtained this way, are also stated in Table I.

IV. DISCUSSION

Figure 3 and the results summarized in Table I, support the validity of the power law (3) with an exponent β that depends only on q, but not on a or N. According to the quoted uncertainties in β (see Table I), we see that the individual exponents are more accurately defined for smaller values of q. The reason for this is straightforward. According to (1), q determines the strength of the ac drive of the trap, which, in turn, determines the degree of chaos in the trap. Therefore, smaller q means less chaos, which implies smaller $\Delta\gamma_c$, which, in turn, results in a better defined β.

According to Fig. 3, for $\gamma - \gamma_c \gtrsim 3 \times 10^{-4}$, the duration $\bar{\tau}_m$ of the metastable state is smaller than 1000 (i.e., smaller than $\approx$300 rf cycles), which, on the scale of Fig. 1, is a very small time interval. In fact, as corroborated by Fig. 1, it is no longer possible in this case to clearly separate the metastable state from the initial thermalization stage. This is expected since, for a relatively large $\gamma > \gamma_c$, the cloud is cooled so fast that the metastability does not have enough time to clearly manifest itself. This provides us with a natural cutoff damping parameter, i.e., $\gamma_{\text{cutoff}}(N,a,q) = \gamma_c(N,a,q) + 3 \times 10^{-4}$, above which metastability can no longer be defined. It also provides us with an estimate for the onset of the power-law behavior, i.e., we expect the power law to hold for $\gamma - \gamma_c \lesssim 3 \times 10^{-4}$. Although, according to (2), γ_{cutoff} depends, via γ_c, on N and both trap control parameters, the dependence on N is weak, especially for large N.

Our results are directly applicable to currently conducted Paul-trap experiments. Our work may, for instance, be used to determine the cooling power and its duration that need to be applied to the charged particles stored in a Paul trap in order to ensure crystallization. Using our results shown in Fig. 3(b), for instance, one can predict that, for a typical rf-frequency of $f = 1$ MHz, a damping constant 5% above the critical damping γ_c results in a metastable-state lifetime of $\bar{\tau}_m \sim 10^4$, or $\approx$3 ms.

In this paper we focused on the cloud $\rightarrow$ crystal transition. But what about crystal $\rightarrow$ cloud transitions? Indeed, these were reported in the experimental [4] as well as in the theoretical [12,13,15] AMO literature. They are, however, of a completely different nature than the phenomena studied in this paper. Corroborating earlier results [3,21], we found that in an ideal Paul trap described by (1), even in the absence of damping (i.e., $\gamma = 0$), crystal $\rightarrow$ cloud transitions do not occur. We checked this fact explicitly for many different a,q combinations, and N ranging from 25 to 200. The explanation is straightforward. There is no chaos in the crystal state. Therefore, crystals do not heat, and are therefore stable even in the absence of damping. In experiments that do observe crystal $\rightarrow$ cloud transitions, the crystals are heated by an outside source, for instance, by coupling to the hot, ambient air in the experiments reported in [4]. Thus, while crystal $\rightarrow$ cloud transitions certainly occur in experiments in which the crystals are coupled to a heat bath, their underlying mechanism is completely different from the self-contained, dynamical transitions studied in this paper.

In addition to radio-frequency traps, widely used in AMO physics, our results and methods are also applicable to a host of many-particle systems in various other areas of physics, which also show Wigner crystallization [33–39]. Of particular importance in our context are crystalline beams [33,34]. This is so, since in their rest frame the dynamics of the beam particles are described by equations very similar to (1), and a phase transition, very similar to the one described in this paper, induced by laser or electron cooling, precedes the transition into the Wigner crystal [42]. We mention that beam crystallization has already been observed in a mini-storage ring [43], an excellent system for testing the universality of our predictions.

V. SUMMARY AND CONCLUSIONS

Summarizing, we showed that for ions stored in a Paul trap, a critical value, $\gamma_c(N,a,q)$, of the damping constant γ exists at which the cloud $\to$ crystal transition occurs. We showed that γ_c scales approximately like $\ln[\ln(N)]$ in the number N of stored particles in the trap. In addition, we showed that close to the cloud $\to$ crystal transition the mean lifetime $\bar{\tau}_m$ of the metastable cloud follows a power law. Many AMO laboratories, nationally and internationally, are equipped to test our predictions. We are confident that our predictions will hold up to experimental tests.

[1] W. Paul, Rev. Mod. Phys. **62**, 531 (1990).
[2] P. K. Ghosh, *Ion Traps* (Clarendon Press, Oxford, 1995).
[3] R. Blümel, J. M. Chen, E. Peik, W. Quint, W. Schleich, Y. R. Shen, and H. Walther, Nature (London) **334**, 309 (1988).
[4] R. F. Wuerker, H. Shelton, and R. V. Langmuir, J. Appl. Phys. **30**, 342 (1959).
[5] I. M. Buluta, M. Kitaoka, S. Georgescu, and S. Hasegawa, Phys. Rev. A **77**, 062320 (2008).
[6] Sh. Amiranashvili, N. Gusein-zade, and A. Ignatov, Phys. Rev. A **59**, 3098 (1999).
[7] I. M. Buluta and S. Hasegawa, Phys. Rev. A **78**, 042340 (2008).
[8] M. G. Raizen, J. M. Gilligan, J. C. Bergquist, W. M. Itano, and D. J. Wineland, Phys. Rev. A **45**, 6493 (1992).
[9] J. I. Cirac and P. Zoller, Phys. Rev. Lett. **74**, 4091 (1995).
[10] J. M. Taylor and T. Calarco, Phys. Rev. A **78**, 062331 (2008).
[11] K. Okada, M. Wada, T. Takayanagi, S. Ohtani, and H. A. Schuessler, Phys. Rev. A **81**, 013420 (2010).
[12] J. W. Emmert, M. Moore, and R. Blümel, Phys. Rev. A **48**, R1757(R) (1993).
[13] A. W. Vogt, Phys. Rev. A **49**, R657(R) (1994).
[14] M. G. Moore and R. Blümel, Phys. Rev. A **50**, R4453(R) (1994).
[15] R. Blümel, Phys. Rev. A **51**, 620 (1995).
[16] E. Wigner, Phys. Rev. **46**, 1002 (1934).
[17] M. A. N. Razvi, X. Z. Chu, R. Alheit, G. Werth, and R. Blümel, Phys. Rev. A **58**, R34(R) (1998).
[18] R. Alheit, X. Z. Chu, M. Hoefer, M. Holzki, G. Werth, and R. Blümel, Phys. Rev. A **56**, 4023 (1997).
[19] J. D. Tarnas, Y. S. Nam, and R. Blümel, Phys. Rev. A **88**, 041401(R) (2013).
[20] Y. S. Nam, E. B. Jones, and R. Blümel, Phys. Rev. A **90**, 013402 (2014).
[21] R. Blümel, C. Kappler, W. Quint, and H. Walther, Phys. Rev. A **40**, 808 (1989).
[22] H. Walther, Adv. At. Mol. Opt. Phys. **31**, 137 (1993).
[23] F. Diedrich, E. Peik, J. M. Chen, W. Quint, and H. Walther, Phys. Rev. Lett. **59**, 2931 (1987).
[24] D. J. Wineland, J. C. Bergquist, W. M. Itano, J. J. Bollinger, and C. H. Manney, Phys. Rev. Lett. **59**, 2935 (1987).
[25] J. Hoffnagle and R. G. Brewer, Phys. Rev. A **50**, 4157 (1994).
[26] L. S. Brown, Phys. Rev. Lett. **66**, 527 (1991).
[27] F. Diedrich, J. C. Bergquist, W. M. Itano, and D. J. Wineland, Phys. Rev. Lett. **62**, 403 (1989).
[28] J. Hoffnagle, R. G. DeVoe, L. Reyna, and R. G. Brewer, Phys. Rev. Lett. **61**, 255 (1988).
[29] J.-L. Shen, H.-W. Yin, J.-H. Dai, and H.-J. Zhang, Phys. Rev. A **55**, 2159 (1997).
[30] H. G. Dehmelt, Adv. At. Mol. Phys. **3**, 53 (1967); **5**, 109 (1969).
[31] K. Chen, S. T. Sullivan, W. G. Rellergert, and E. R. Hudson, Phys. Rev. Lett. **110**, 173003 (2013).
[32] D. S. Goodman, J. E. Wells, J. M. Kwolek, R. Blümel, F. A. Narducci, and W. W. Smith, Phys. Rev. A **91**, 012709 (2015).
[33] J. P. Schiffer and P. Kienle, Z. Phys. A **321**, 181 (1985).
[34] Y. Yuri and H. Okamoto, Phys. Rev. ST Accel. Beams **8**, 114201 (2005).
[35] H. Thomas, G. E. Morfill, V. Demmel, J. Goree, B. Feuerbacher, and D. Möhlmann, Phys. Rev. Lett. **73**, 652 (1994).
[36] T. E. Sheridan, Phys. Plasmas **12**, 080701 (2005).
[37] Edited by E. Y. Andrei, *Two-Dimensional Electron Systems* (Kluwer Academic, Dordrecht, 1997).
[38] E. R. Russell, F. Spaepen, and D. A. Weitz, Phys. Rev. E **91**, 032310 (2015).
[39] E. Tjhung and Ludovic Berthier, Phys. Rev. Lett. **114**, 148301 (2015).
[40] W. H. Press, S. A. Teukolsky, W. T. Vetterling, and B. P. Flannery, *Numerical Recipes in C*, 2nd ed. (Cambridge University Press, Cambridge, 1992).
[41] We compute a moving average of $\langle x^2 \rangle_{\Delta t}$ (averaging over a time interval $[t - \Delta t, t + \Delta t]$), which yields very sharp transitions suitable for an automatic and objective extraction of τ_m via a computer program. The choice of the interval Δt, which is of the order of the temporal transition width of the cloud $\to$ crystal transition, is not critical.
[42] H. Primack and R. Blümel, Phys. Rev. E **58**, 6578 (1998).
[43] T. Schätz, U. Schramm, and D. Habs, Nature (London) **412**, 717 (2001).